Environment Canada

Water Science and Technology Directorate

Direction générale des sciences et de la technologie, eau

Environnement Canada

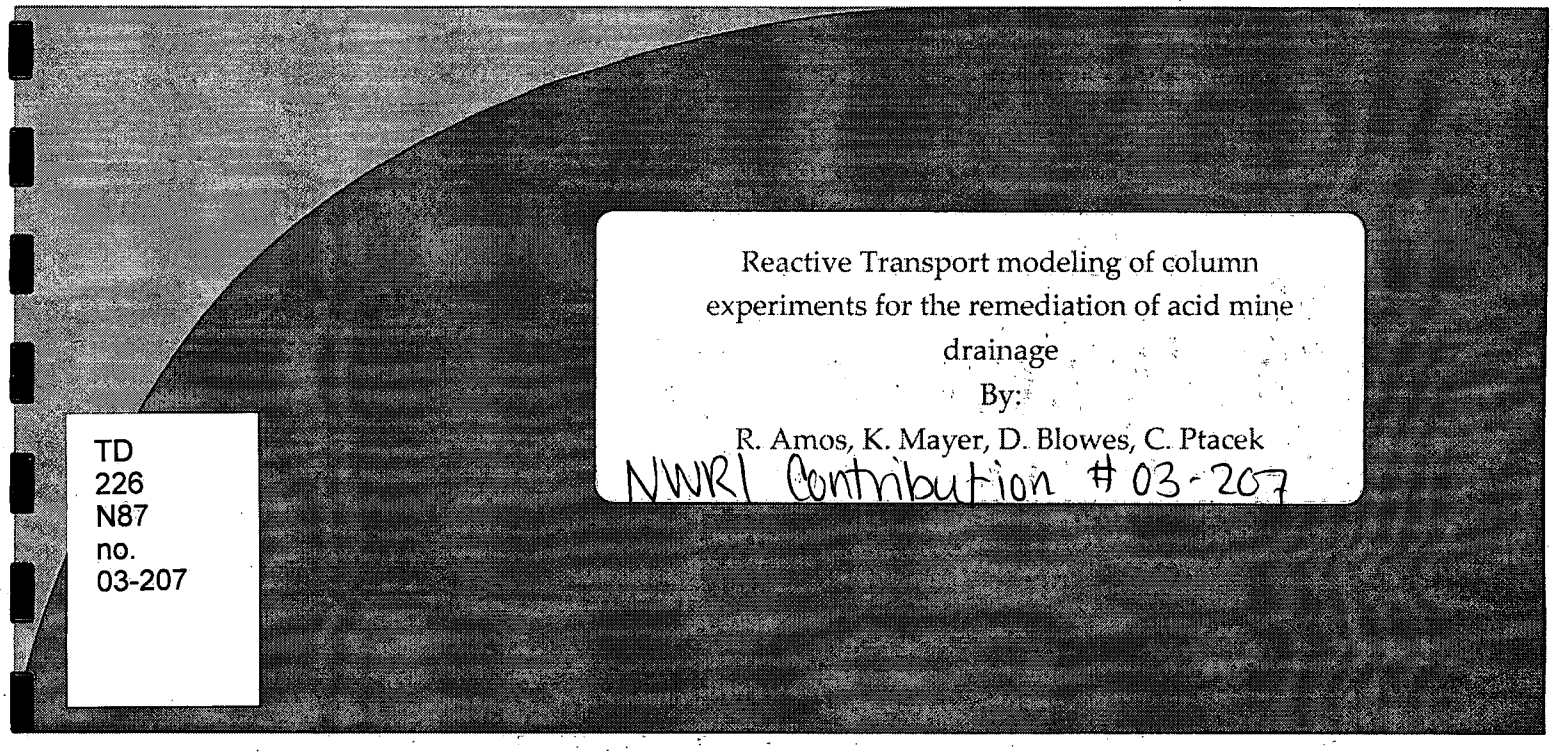

Reactive Transport modeling of column experiments for the remediation of acid mine drainage

By:

R. Amos, K. Mayer, D. Blowes, C. Ptacek

03-207

Reactive Transport Modeling of Column Experiments for the Remediation of Acid Mine Drainage

Richard T. Amos, K. Ulrich Mayer, David W. Blowes, and Carol J. Ptacek

Abstract

Reactive transport modeling was used to evaluate the performance of two similar column experiments. The experiments were designed to simulate the treatment of acid mine drainage through microbially mediated sulfate reduction and subsequent sulfide mineral precipitation by means of an organic carbon permeable reactive barrier. Principal reactions considered in the simulations include microbially-mediated reduction of sulfate by organic matter, mineral dissolution/precipitation reactions and aqueous complexation/hydrolysis reactions. Simulations of Column 1, which contained composted leaf mulch, wood chips, sawdust, and sewage sludge as an organic carbon source, accurately predicted sulfate concentrations in the column effluent throughout the duration of the experiment using a single fixed rate constant for sulfate reduction of 6.5×10^{-9} mol L^{-1} s^{-1}. Using the same reduction rate for Column 2, which contained only composted leaf mulch and sawdust as an organic source, sulfate concentrations at the column outlet were over-predicted at late times suggesting that sulfate reduction rates increased over the duration of the column experiment and that microbial growth kinetics may have played an important role. These modeling results suggest that the reactivity of the organic carbon treatment material with respect to sulfate reduction does not significantly decrease over the duration of the fourteen-month experiments. The ability of the columns to remove ferrous iron appears to be strongly influenced by the precipitation of siderite, which is enhanced by the dissolution of calcite. The simulations indicate that while calcite was available in the column, up to 0.02 mol L^{-1} of ferrous iron where removed from solution as siderite and mackinawite. Later in the experiments after ~300 days, when calcite was depleted from the columns, mackinawite became the predominant iron sink. The ability of the column to remove ferrous iron as mackinawite was estimated to be ~0.005 mol L^{-1} for Column 1. As the precipitation of mackinawite is sulfide limited at later times the amount of iron removed will ultimately depend on the reactivity of the organic mixture and the amount of sulfate reduced.

Key Words: Acid Mine Drainage, Permeable Reactive Barrier, Sulfate Reduction, Reactive Transport Modeling

NWRI RESEARCH SUMMARY

Plain language title
Application of a computer model for designing groundwater remediation systems at contaminated mine sites.

What is the problem and what do sicentists already know about it?
Large volumes of waste rock and tailings are created as a result of ore removal. These wastes are usually deposited in piles or in impoundments in the vicinity of the mine. Over time the wastes weather, leading to the release of metals, acid and sulfate to the environment. The release usually occurs over many decades to centuries. At many of these sites, large plumes of contaminated groundwater have developed. This groundwater is now flowing toward adjacent rivers and lakes where it will eventually discharge. In Canada, there are over 10,000 abandoned mine sites, therefore low cost abatement techniques are required to prevent the release of contaminants, including low cost systems for addressing groundwater contamination. A number of remediation systems have been developed to prevent the discharge.

Why did NWRI do this study?
This study was carried out to use bench-scale data to develop a predictive model that can be used to assess and design groundwater remediation systems over the long operation time that is required at many mine sites. The model incorporates kinetic rate constants to simulate the long-term reactivity of organic-carbon based reactive media. This media acts as a bacterial substrate for promoting sulfate reducing conditions and the passive removal of metals, sulfate and acid from groundwater. The kinetic parameters obtained from the model can be used as design parameters for full-scale treatment systems.

What were the results?
The model was applied to two bench-scale column experiments which contained organic carbon mixtures to induce sulfate reducing conditions and enhance contaminant removal. The calculations were in excellent agreement with the observed changes in water chemistry.

How will these results be used?
The results can be used to delineate reaction mechanisms and rate constants for making long-term predictions of system performance.

Who were our main partners in the study?
The Canadian Water Network, University of British Columbia, and the University of Waterloo

Modélisation du transport en milieu réactif par des essais sur colonne, pour l'assainissement des eaux d'exhaure acides

Richard T. Amos, K. Ulrich Mayer, David W. Blowes et Carol J. Ptacek

Résumé

On a utilisé la modélisation du transport en milieu réactif pour évaluer la performance de deux essais sur colonne semblables, conçus pour simuler le traitement des eaux d'exhaure acides par une réduction microbienne du sulfate, suivie par la précipitation du sulfure inorganique à l'aide d'une barrière réactive perméable de carbone organique. Les principales réactions examinées au cours des simulations sont notamment des réactions microbiennes de réduction du sulfate par des matières organiques, des réactions de dissolution et de précipitation des minéraux et des réactions aqueuses de complexation et d'hydrolyse. Les simulations avec la colonne 1, qui contenait du paillis de feuilles compostées, des copeaux de bois, de la sciure et des boues d'eaux usées comme source de carbone organique, ont permis de prévoir avec précision les concentrations de sulfate à la sortie de la colonne pendant toute la durée de l'essai, avec une seule constante de vitesse pour la réduction du sulfate ($6{,}5 \times 10^{-9}$ mol L^{-1} s^{-1}). Avec cette même constante de vitesse de réduction pour la colonne 2, qui ne contenaient que du paillis de feuilles compostées et de la sciure de bois comme source de matières organiques, les prévisions relatives aux concentrations de sulfate à la sortie de la colonne étaient trop élevées vers la fin, ce qui semble indiquer une augmentation des vitesses de réduction du sulfate en fonction de la durée de l'essai sur colonne, ainsi qu'un rôle important possible de la cinétique de croissance des agents microbiens. Ces résultats laissent donc croire que, pour ce qui est de la réduction du sulfate, la réactivité du substrat de traitement à base de carbone organique ne diminue pas de façon notable au cours de la période d'essais de quatorze mois. De plus, la capacité des colonnes à éliminer le fer ferreux semble fortement influencée par la précipitation de la sidérite, qui est améliorée par la dissolution de la

calcite. Les simulations indiquent que, pendant que la calcite était disponible dans la colonne, on obtenait une élimination de jusqu'à 0,02 mol L^{-1} du fer ferreux de la solution, sous forme de sidérite et de mackinawite. Vers la fin de la période d'essai (après environ 300 jours), après l'épuisement de la calcite, c'est la précipitation de mackinawite qui est devenue le principal mécanisme d'élimination du fer. Pour la colonne 1, on a évalué à environ 0,005 mol L^{-1} la capacité de la colonne à éliminer le fer ferreux sous forme de mackinawite. Étant donné que, vers la fin de l'essai, la précipitation de la mackinawite était limitée par la concentration du sulfure, la quantité de fer éliminée dépendait de la réactivité du mélange de composés organiques et de la quantité de sulfate réduit.

Mots-clés: eaux d'exhaure acides, barrière réactive perméable, réduction du sulfate, modélisation du transport en milieu réactif

Sommaire des recherches de l'INRE

Titre en langage clair
Application d'un modèle informatique à la conception de systèmes d'assainissement des eaux souterraines aux sites miniers contaminés

Quel est le problème et que savent les chercheurs à ce sujet?
L'extraction du minerai produit de grandes quantités de stériles et de résidus, qui sont généralement entassés ou stockés dans des bassins de retenue à proximité de la mine. Avec le temps, ceux-ci s'altèrent sous l'effet des conditions météorologiques, ce qui entraîne la libération de métaux, d'acides et de sulfates dans l'environnement, habituellement sur une période allant de plusieurs décennies à des siècles. D'importants panaches d'eau souterraine contaminée se sont formés dans beaucoup de sites miniers. Cette eau s'écoule maintenant en direction de cours d'eau et de lacs voisins, où elle finira par s'introduire. Il y a plus de 10 000 mines abandonnées au Canada; il faut donc utiliser des techniques peu coûteuses de réduction de la pollution pour empêcher le rejet de contaminants dans les milieux naturels, y compris des systèmes économiques de décontamination des eaux souterraines. Un certain nombre de systèmes d'assainissement ont été mis au point pour prévenir les rejets.

Pourquoi l'INRE a-t-il effectué cette étude?
L'étude avait pour objet d'utiliser des données d'essai en laboratoire afin d'élaborer un modèle de prévision permettant d'évaluer et de concevoir des systèmes d'assainissement des eaux souterraines pouvant fonctionner sur la longue période d'utilisation nécessaire à de nombreux sites miniers. Le modèle intègre des constantes cinétiques qui permettent de simuler la réactivité à long terme de milieux actifs à base de carbone organique. Ces

milieux agissent comme substrats bactériens favorisant l'établissement de conditions propices à la réduction des quantités de sulfates et la suppression passive des métaux, des sulfates et des acides des eaux souterraines. Les paramètres cinétiques obtenus de la modélisation peuvent servir de paramètres de calcul pour la mise au point de systèmes de traitement en vraie grandeur.

Quels sont les résultats?
Le modèle a été utilisé dans deux expériences de laboratoire en colonnes contenant des mélanges à base de carbone organique visant à produire des conditions propices à la réduction des volumes de sulfates et à accroître la suppression des contaminants. Les calculs concordaient très étroitement avec les changements observés dans la chimie de l'eau.

Comment ces résultats seront-ils utilisés?
Les résultats peuvent servir à établir des mécanismes de réaction et des constantes de vitesse permettant de réaliser des prévisions à long terme de la performance des systèmes.

Quels étaient nos principaux partenaires dans cette étude?
Réseau canadien de l'eau, Université de la Colombie-Britannique et Université de Waterloo.

Reactive Transport Modeling of Column Experiments for the Remediation of Acid Mine Drainage

Richard T. Amos,[*,†] K. Ulrich Mayer,[†] David W. Blowes,[‡] and Carol J. Ptacek [‡,§]

Dept. Earth and Ocean Sciences, Univ. British Columbia, Vancouver, BC, V6T 1Z4, Canada

Dept. Earth Sciences, Univ. Waterloo, Waterloo, ON, N2L 3G1, Canada

and

National Water Research Institute, Environment Canada, Burlington, ON, L7R 4A6, Canada

---

[*] Corresponding author phone: (604)822-6080; fax (604)822-6088; email; ramos@eos.ubc.ca

[†] University of British Columbia

[‡] University of Waterloo

[§] National Water Research Institute

Abstract

Reactive transport modeling was used to evaluate the performance of two similar column experiments. The experiments were designed to simulate the treatment of acid mine drainage through microbially mediated sulfate reduction and subsequent sulfide mineral precipitation by means of an organic carbon permeable reactive barrier. Principal reactions considered in the simulations include microbially-mediated reduction of sulfate by organic matter, mineral dissolution/precipitation reactions and aqueous complexation/hydrolysis reactions. Simulations of Column 1, which contained composted leaf mulch, wood chips, sawdust, and sewage sludge as an organic carbon source, accurately predicted sulfate concentrations in the column effluent throughout the duration of the experiment using a single fixed rate constant for sulfate reduction of 6.5×10^{-9} mol L^{-1} s^{-1}. Using the same reduction rate for Column 2, which contained only composted leaf mulch and sawdust as an organic source, sulfate concentrations at the column outlet were over-predicted at late times suggesting that sulfate reduction rates increased over the duration of the column experiment and that microbial growth kinetics may have played an important role. These modeling results suggest that the reactivity of the organic carbon treatment material with respect to sulfate reduction does not significantly decrease over the duration of the fourteen-month experiments. The ability of the columns to remove ferrous iron appears to be strongly influenced by the precipitation of siderite, which is enhanced by the dissolution of calcite. The simulations indicate that while calcite was available in the column, up to 0.02 mol L^{-1} of ferrous iron where removed from solution as siderite and mackinawite. Later in the experiments after ~300 days, when calcite was depleted from the columns, mackinawite became the predominant iron sink. The ability of the column to remove ferrous iron as mackinawite was estimated to be ~0.005 mol L^{-1} for Column 1. As the precipitation of mackinawite is sulfide

limited at later times the amount of iron removed will ultimately depend on the reactivity of the organic mixture and the amount of sulfate reduced.

Key Words:

Acid Mine Drainage, Permeable Reactive Barrier, Sulfate Reduction, Reactive Transport Modeling,

Introduction

Groundwater contamination from mine tailings impoundments is often characterized by high concentrations of SO_4, Fe(II) and other metals, and a near neutral pH (*1, 2*). Left untreated the ferrous iron in contaminated groundwater will be oxidized to ferric iron upon discharge to oxygenated surface water and the subsequent precipitation of ferric oxyhydroxides would produce acidic conditions with detrimental effects to the ecosystem.

One currently employed treatment technique is the use of an organic carbon permeable reactive barrier to stimulate sulfate reduction and subsequent metal sulfide precipitation (*3, 4*). The reduction of sulfate by organic carbon can be represented by the equation;

$$2CH_2O + SO_4^{2-} \rightarrow 2HCO_3^- + H_2S \qquad (1)$$

where CH_2O represents short chain organic carbon molecules which are capable of being oxidized by sulfate reducing bacteria. The sulfides produced from the above reaction form sparingly soluble sulfide minerals;

$$Me^{2+} + H_2S \rightarrow MeS_{(solid)} + 2H^+ \qquad (2)$$

where Me^{2+} represents divalent metal cations such as Fe^{2+}, Zn^{2+} and Ni^{2+}.

Column experiments were previously run to simulate the treatment of acid mine drainage contaminated groundwater and assess the rates of sulfate reduction and metal removal of selected organic carbon mixtures (*5, 6*). Two columns were constructed consisting of a reactive mixture containing creek sediment as a bacterial source, limestone as a neutralizing agent, silica sand as a non-reactive porous medium, and an organic carbon source which consisted of composted leaf mulch, wood chips, sawdust, and sewage sludge. The column input solution was simulated acid mine drainage comparable in characteristics to the Nickel Rim plume (*2*).

At the Nickel Rim mine site near Sudbury, Ontario a full-scale reactive barrier was installed to treat ground water emanating from the tailings impoundment. The barrier, which was installed in 1995, was shown to reduce sulfate and decrease down-gradient metal loading (*3*). The reactive transport code MIN3P (*7*) was used to model physical heterogeneities and temporal variations in temperature that impact the performance of the Nickel Rim barrier (*8, 9*).

Here we use MIN3P to simulate the remediation process from the more controlled conditions of the column experiments (*5,6*). The focus of the present study is to test the existing conceptual model using reactive transport modeling based on the detailed dataset obtained from the column influent and effluent chemistry. An additional goal of this study is to investigate the effects of changes in organic matter reactivity, sulfate reduction rates, and mineralogical assemblage within the treatment material on the long-term metal removal capability of the reactive mixture.

Conceptual Model

The conceptual model is based on the column experiments described in Waybrant (*5*) and Waybrant et al. (*6*) and on field studies of the full-scale permeable barrier at the Nickel Rim site by Benner et al. (*3, 10-12*) and Herbert et al. (*13*). In the reactive medium sulfate is reduced by organic carbon to produce sulfide and carbonate according to Reaction 1 in Table 1. Microbiological studies and sulfur isotope data confirm that this is a bacterially mediated reaction (10), although the model does not currently consider bacterial growth and decay, uptake of nutrients or by-products of bacterial organic decay such as phosphate. Furthermore, the reactivity of the organic matter is considered to be constant.

The model assumes all sulfate is reduced to sulfide, which either forms an aqueous sulfide species or precipitates in the form of metal sulfides. However, mineralogical studies

suggest that native sulfur and/or pyrite may also form in the reactive medium (*13*). A possible reaction pathway involves the reduction of sulfate to sulfide followed by oxidation of the sulfide to form sulfur species of intermediate redox states (*14*). This is supported by bacterial studies at the Nickel Rim barrier that show elevated numbers of sulfide oxidizing bacteria within the reactive media (*11*). It is unclear what oxidant is available in the barrier to facilitate this reaction.

Boudreau and Westrich (*15*) show that the rate of sulfate reduction by organic matter in marine sediments is dependent on the concentration of sulfate only when sulfate concentrations are low. They use a Monod type rate expression of the form;

$$R = k_m \frac{[SO_4]}{K_S + [SO_4]} \qquad (3)$$

where R is the sulfate reduction rate, k_m is the maximum rate, and K_S is the half saturation constant equal to 1.62mM. For SO_4 concentrations significantly above 1.62mM, R is essentially constant and the rate of sulfate reduction is independent of sulfate concentrations.

In response to the changes in geochemistry of the water due to sulfate reduction a number of mineral precipitation and dissolution reactions occur. In addition to the precipitation of iron sulfides, the formation of iron carbonates occurs due to the increase in dissolved carbonate. The solubility of mackinawite (FeS) is much lower than that of siderite ($FeCO_3$) and ultimately controls the concentration of ferrous iron in solution provided sufficient sulfide is present. The nickel and zinc sulfide minerals, millerite and sphalerite respectively, will also become oversaturated within the reactive medium and precipitate. The co-precipitation of nickel and zinc with iron sulfides is not considered in the model. The concentrations of these metals in solution is much lower than iron so that these minerals are less important in terms of controlling the overall aqueous chemistry in the pore water.

Experimental data show a significant increase in calcium concentrations in the column indicating a source of calcium within the reactive mixture (*5, 6*). The reactive mixture contains limestone, which is potentially dissolving in response to geochemical changes in the pore water, including decreases in carbonate concentration from siderite precipitation and changes in pH. Gypsum may also be present in the column as a result of the column preparation techniques. In the current simulation gypsum was not added to the reactive mixture but was allowed as a secondary phase.

The pH in the system is controlled by the complex interaction between the sulfate reduction reactions, the mineral precipitation and dissolution reactions noted above and speciation reactions. Column effluent pH initially starts at approximately 7.0 and decreases to 6.5 over the length of the experiment. In terms of proton balance, this is a small increase over influent pH which varies from 6.0 to 6.5 (*5, 6*).

Model Parameters

The experiments were run in 40 cm long columns, 5 cm in diameter with a 5 cm silica sand layer at the influent end and a 1.5 cm silica sand layer at the effluent end. The remainder of the columns contained reactive mixtures as outlined in Table 2 (*5, 6*). The columns were modeled with a 40 cm long one-dimensional solution domain discretized into 40, 1 cm control volumes. The volume fractions of calcite were set to 0.0031 for column 1 and 0.0036 for column 2 which is representative of the volume in the columns but was adjusted to fit model data as described below. For organic carbon the volume fraction was arbitrarily set to 0.1 to represent the amount of the readily degradable organic carbon in the mixture. In this case the volume fraction of the organic carbon was sufficiently high so that the reaction progress was not limited by the availability of organic material. The remainder of the solid phase in the reactive mixture is

considered to be non-reactive, as are the silica sand layers. Physical properties used in the model are listed in Table 3 and are homogeneous throughout the entire solution domain. All properties are those measured from the column experiments (*5, 6*). The simulations were run for a 425 day period which approximately corresponds to the length of time the column experiments were run.

The following 17 components are used to describe the geochemical system: Ar(aq), Br, Ca, CO_3, Cl, Fe(II), H^+, H_2S, K, Mg, Mn, Na, Ni, O_2(aq), S, SO_4, and Zn. Based on the WATEQ4F (*16*) and MINTEQA2 (*17*) databases 76 aqueous species were identified and included in the model to accurately determine mineral solubilities.

The sulfate reduction reaction (Reaction 1, Table 1) is assumed to be a kinetically controlled irreversible reaction, limited by the availability of sulfate, and is modelled with a Monod type rate expression of the form;

$$R_{CH_2O-SO_4} = -k_{CH_2O-SO_4}\left[\frac{[SO_4]}{K_s + [SO_4]}\right] \qquad (4)$$

where $k_{CH_2O-SO_4}$ is the effective constant and K_s is the half saturation constant. The rate constant given in Table 1 was calibrated to match the observed sulfate concentrations from the column data. The half-saturation constant is that determined by Boudreau and Westrich (*15*) for sulfate reduction in marine sediments. The calibrated rate constant, equivalent to 194 mmol SO_4 L^{-1} H_2O yr^{-1}, compares favourably with values determined from the column experiments, 186 mmol SO_4 L^{-1} H_2O yr^{-1} (*6*), but is somewhat higher than that determined for the full scale barrier at Nickel Rim, 47 mmol SO_4 L^{-1} H_2O yr^{-1} (*12*). The lower rate in the field may be due to a lower temperature, ~9 °C (*12*), compared to the column experiments which were conducted at room temperature (*6*).

Mineral dissolution and precipitation reactions are modelled as kinetically controlled reversible reactions with a rate expression of the following form;

$$R = -k_{eff}\left(1 - \frac{IAP}{K}\right) \qquad (5)$$

where k_{eff} is the effective rate constant for the dissolution of the mineral phase, IAP is the ion activity product and K is the equilibrium constant. Model parameters are shown in Table 1. Effective rate constants are calibrated to match the observed data. Equilibrium constants are from the WATEQ4F (*16*) and MINTEQA2 (*17*) databases.

The column input water chemistry shown in Table 4 (*5, 6*) was used for input boundary conditions. Note that from 0 to 96 days the input solution contained only high sulfate and the simulated acid mine drainage was not used as input solution until after 96 days or 4.7 pore volumes. During feed 1 bromide was added to the input solution for the purposes of a tracer test.

Results and Discussion

Tracer tests

Column effluent breakthrough curves for bromide from the model simulations and the column experiments, shown in Figure 1, show good agreement. This indicates that the model accurately simulates flow conditions using measured values of physical parameters from the column experiments (Table 3).

Sulfate reduction and iron removal: Column 1

Breakthrough curves of modelled effluent sulfate concentrations compared to column influent and effluent sulfate concentrations for Column 1 are shown in Figure 2. Both the column effluent and modelled effluent sulfate concentrations show a decrease over influent sulfate

concentrations as is expected due to sulfate reduction. The rate constant for sulfate reduction in the model was calibrated to provide a best fit for this data and was kept constant over the entire simulation period. The modelled data show a good fit to the column data throughout the 425 day period, indicating that the reactivity of the organic matter does not decrease significantly over time.

Simulated sulfide concentrations show a good fit to the column data where experimental data is available (Figure 2). Sulfide concentrations are controlled by the amount of sulfide produced from sulfate reduction (Equation 1, Table 1) minus the amount of sulfide removed through metal sulfide precipitation (Equations 3, 7 and 8, Table 1). The decreasing trend in sulfide is therefore due to a decrease in sulfate reduction or an increase in metal sulfide precipitation. However, the rate constant for sulfate reduction is constant, and through most of the simulation the concentration of sulfate remains well above the half saturation constant (with the exception of the first 100 days). Therefore the rate of sulfate reduction and the amount of sulfide produced is constant throughout most of the simulation. Furthermore, the concentrations of Ni and Zn are very low and the amount of millerite and sphalerite precipitation will not significantly affect aqueous sulfide concentrations. The decreasing trend in sulfide concentrations must therefore be predominantly due to an increase in the amount of iron sulfide precipitation over the course of the experiment. The mechanism by which mackinawite precipitation increases over time will be discussed in detail below. Another possible mechanism of sulfide removal, which is not considered in the model, is the oxidation of sulfide resulting in the formation of native sulfur or pyrite.

Modelled ferrous iron concentrations show a good fit to column data. Both modelled and column effluent data show a significant decrease in the ferrous iron concentrations over influent

data due to mackinawite and siderite precipitation. However, initially (up to ~250 days) all ferrous iron is removed from solution, equivalent to ~0.015 mol L^{-1}, while at later times (after ~250 days) ferrous iron remains in the effluent and the amount removed is only ~0.005 mol L^{-1}. Therefore, the rate of iron removal decreases substantially as the column experiments progress.

The decrease in sulfide concentration and the increase in ferrous iron concentrations in the column effluent through the duration of the experiments can be examined through the use of modelled spatial profiles at various times. Figure 3A shows spatial profiles of total aqueous component concentrations for Fe(II), SO_4, and H_2S at 150 days while Figure 3B shows dissolution and precipitation rates for various minerals at the same time. Sulfate concentrations show a steady decrease throughout the profile due to sulfate reduction. Concentrations remain well above the half saturation constant throughout the profile indicating that the sulfate reduction rate, and therefore sulfide production, will remain nearly constant throughout the column. A linear trend would be expected for a constant sulfate reduction rate however changes in input concentrations (Figure 3A) and dissolution and precipitation of gypsum (Figure 3B) produces deviations from the linear trend.

Sulfide concentrations remain low initially in the column due to mackinawite precipitation and begin to increase at 0.2 m, once mackinawite precipitation rates decline (Figures 3A and 3B). Mackinawite is initially oversaturated in the column due to high influent concentration of ferrous iron and the production of sulfide. However, due to the complete removal of Fe(II) at approximately 0.2 m, mackinawite is no longer oversaturated and precipitation ceases. Ferrous iron levels are controlled by both mackinawite and siderite precipitation although as is seen in Figure 3B the rate of precipitation for siderite is much greater

than that of mackinawite and therefore siderite is the predominant sink for ferrous iron at this point in time.

Siderite solubility is controlled by carbonate and ferrous iron concentration. The precipitation of siderite consumes carbonate leading to undersaturation with respect to calcite, which causes calcite to dissolve and liberates more carbonate. The net result is the mutual enhancement of the two processes resulting in increased siderite precipitation, enhanced iron removal, increased calcite dissolution and increased dissolved calcium concentrations. As is seen in Figures 3A and B the precipitation of siderite and the dissolution of calcite cease at 0.2 m as the ferrous iron concentrations approach zero. Likewise, these processes begin at 0.1 m which corresponds to the point in the column where calcite exists. At 150 days calcite has been depleted in the column from 0 to 0.1 m due to dissolution.

With respect to ferrous iron and sulfide concentration the above discussion can be summarized as follows. Iron concentrations are controlled by both siderite and mackinawite precipitation, however, the majority of the iron is removed through siderite precipitation. In turn siderite precipitation is enhanced by calcite dissolution and controlled by the availability of calcite in the column. Sulfide production is constant throughout the column but concentrations of sulfide are controlled by mackinawite precipitation. At 150 days mackinawite precipitation is iron limited, due to the removal of iron from siderite precipitation, and therefore column effluent contains dissolved sulfide.

Figures 3C and 3D show spatial profiles through the column at 200 days. The patterns observed are very similar to those seen at 150 days (Figures 3A and 3B). However, in this case siderite precipitation and calcite dissolution occur much closer to the outflow end of the column, ~0.2 to 0.3m. The delay in the commencement of these processes is due to the depletion of

calcite in the column up to ~0.2m. This causes ferrous iron concentrations to remain high through most of the column allowing mackinawite precipitation to continue through a longer portion of the column. Mackinawite precipitation is still iron limited in this case, however, more sulfide is removed resulting in a lower sulfide concentration in the column effluent (see also Figure 2).

The spatial profiles at 300 days are shown in Figures 3E and F. The most notable difference compared to earlier profiles is that siderite precipitation does not proceed to any significant degree. This is because calcite is now completely dissolved from the column. The result in this case is that iron levels remain relatively high throughout the column and mackinawite precipitation is no longer limited by ferrous iron. Mackinawite precipitation then continues throughout the column and sulfide concentrations approach zero, as is observed in the column effluent (Figure 2).

As was noted above, the amount of solid-phase calcite included in the simulations was adjusted to fit the data. As no analysis of solid phase calcite was done on the columns the availability of calcite at various times cannot be verified. However, other evidence suggests that calcite dissolution is occurring in the column and calcite is exhausted from the column at ~300 days. Breakthrough curves of modelled effluent calcium concentrations compared to column influent and effluent calcium concentrations for Column 1 are shown in Figure 4. Both modelled and column effluent calcium concentrations show a significant increase over influent concentration in the period from ~100 to 300 days which corresponds to the time period when model results indicate that calcite is dissolving and iron is removed by siderite precipitation. Although the concentrations of calcium in the modelled and column data do not agree exactly the general trends are very similar. The discrepancy in the calcium concentration is likely due to the

difficulties in simulating pH and its effect on carbonate speciation, as described below. Furthermore, at later times (>300 days) calcium influent and effluent concentrations are equal indicating that no source of calcium exists and that calcite is no longer dissolving. This corresponds to the period of time when the model results suggest that calcite is depleted from the column.

In addition, simple mass balance calculations indicate that the amount of sulfide produced cannot account for the large decrease in ferrous iron in the column through mackinawite precipitation alone. For example, at 150 days ~0.01 mol L^{-1} sulfate are removed from solution (Figure 2). Using the stoichiometry of Equations 1 and 3 in Table 1, 1 mole of sulfate produces 1 mole of sulfide, which will precipitate with 1 mole of ferrous iron to produce 1 mole of mackinawite. At this time ~0.005 mol L^{-1} sulfide remains in the column effluent indicating that only ~0.005 mol L^{-1} sulfide is used for mackinawite precipitation. However, ~0.02 mol L^{-1} of ferrous iron is removed from solution which suggests that ~0.015 mol L^{-1} ferrous iron is removed via an alternate sink.

The pH data from the model simulations and the column data (*5, 6*) are shown in Figure 4B. The model under-predicts pH at all times and more significantly at later times suggesting some discrepancy in the conceptual model. Inconsistencies in the conceptual model may arise from the simplified approach to the sulfate reduction reactions. These reactions involve the decomposition of complex organic matter that contains other compounds such as ammonia and phosphate. Column effluent was sampled for ammonium and phosphate and did not show any increase in the amount of ammonium but did show phosphate concentrations up to 10 mg/L (*5*). It is unclear how this would affect the pH of the effluent water. Furthermore, the production of intermediate sulfur redox species is not considered in the model. As an example, the oxidation of

the sulfide to sulfur by goethite, potentially a constituent of the sediment included in the column, is as follows;

$$H_2S + 2FeOOH_{(s)} + 4H^+ \rightarrow S_{(s)} + 2Fe^{2+} + 4H_2O \quad (6)$$

Comparison of this reaction to Reaction 1 in Table 1 shows that this reaction pathway consumes protons whereas the reduction of sulfate to sulfide is neutral as written. Initial model simulations considering the re-oxidation of sulfide to sulfur by goethite have shown that this pathway does have the effect of raising pH.

Nickel, zinc and other cations

Both Ni and Zn concentrations quickly decrease in the column as is shown in Figure 5A. The removal of these trace metals is simulated by the precipitation of millerite and sphalerite, although, it is likely that co-precipitation with iron sulfides occurred in the column experiment instead of, or in addition to these precipitation reactions. Millerite and sphalerite are very insoluble minerals and precipitate quickly with small amounts of sulfide present (Figure 5B). Experimental data (*5*) shows that manganese is removed from the column up to ~250 days, corresponding to the time period when calcite is dissolving in the column (Figure 4), and suggesting that the precipitation of rhodochrosite ($MnCO_3$) is a potential sink for manganese. The simulations do not indicate that precipitation of rhodochrosite is occurring but do show that rhodochrosite approaches saturation near the column effluent. The discrepancy in the simulated pH, i.e. lower simulated pH than observed, would have the effect of increasing the solubility of rhodochrosite and could account for this inconsistency in the model. Manganese concentrations are low in the column experiments and will not significantly affect the overall geochemistry of the system. Other cations such as sodium, magnesium and potassium are unreactive in the simulations which is consistent with the column data (*5, 6*).

Column 2

Breakthrough curves of simulated effluent sulfate concentrations compared to observed column influent and effluent sulfate concentrations for Column 2 are shown in Figure 6A using the same rate constant for sulfate reduction, 6.9×10^{-9} mol L^{-1} bulk day^{-1}, as was calibrated with Column 1. The simulated data show a reasonably good fit to the observed data initially but over-predicts sulfate concentrations at later times. This may suggest that the sulfate reduction rate in the column experiment is increasing with time. A possible explanation is that microbial population growth needs to be considered. Bacterial populations are potentially growing during the initial stages of the experiment and do not reach their maximum until beyond approximately 150 days. Currently the model does not consider microbial growth. Figure 6B shows the results of a simulation run with a sulfate reduction rate constant of 1.5×10^{-8} mol L^{-1} bulk day^{-1}. This rate constant produces a better fit to the later sulfate data, suggesting a maximum sulfate reduction rate constant, but also over-predicts sulfide at all times.

Although the simulations for Column 2 were unable to exactly reproduce the observed trends, the general agreement, specifically the decline in sulfide concentration, the increase in ferrous iron concentrations and the increase in calcium concentrations (data not shown), would tend to indicate that the conceptual model used is a reasonable representation of the geochemical system in the column.

Implications for Long Term Performance

In this modelling study a fixed rate constant was used for sulfate reduction throughout the simulation period. For Column 1 this fixed rate was adequate for reproducing the sulfate concentrations throughout the experiment suggesting that the sulfate reduction rate and the reactivity of the organic matter was not significantly decreasing. The modelling results for

Column 2 indicate that the sulfate reduction rate increased through the experiment, suggesting that microbial population growth may be occurring, but again indicating no significant decrease in sulfate reduction rate. These observations are contrary to the models described by Westrich and Berner (*18*) and Tarutis and Unz (*19*). These models suggest an initially high organic matter degradation rate, which declines quickly as the labile fraction of organic matter is used up; this is not observed in the column data. Without a clear pattern of organic matter degradation in our simulations it is difficult to comment on the expected long-term evolution of the biogeochemical system. It is apparent however that the reactivity of the organic matter did not decrease over the duration of the experiments.

Reactive transport simulations can be used to demonstrate the relationship between sulfate loading and consumption of organic matter. Intuitively it might be expected that an increase in sulfate entering the system, through higher influent concentrations or an increased flow rate, would increase the amount of organic matter consumed. However, this is only the case when sulfate concentrations in the column approach the value of the half saturation constant, K_s, and the Monod expression (Equation 3) essentially becomes a first order rate expression. If sulfate concentrations remain well above K_s the rate is zero order with respect to sulfate and the maximum rate, k_m, is maintained.

This relationship is demonstrated in Figure 7A, which shows spatial profiles of sulfate reduction rates at 200 days for five separate simulations with different flow velocities to represent various rates of sulfate loading. For each of the simulations the velocity was kept constant. The simulations were identical to those conducted for Column 1, except that the influent concentrations were set to the values of Feed 0 (Table 1) and kept constant throughout the simulations. Simulations were conducted with water velocities ranging from 0.0018 m day^{-1}

to 0.09 m day^{-1}, which span the range of water velocities used in the column experiments, 0.018 m day^{-1} to 0.027 m day^{-1}. At the fastest rate, the sulfate loading is high, sulfate concentrations remain high throughout the length of the column, and the sulfate reduction rate is essentially constant. For the slowest rate, sulfate concentrations drop off quickly and the sulfate reduction rate drops to near zero approximately half way through the column.

The effect of the variation in sulfate loading and sulphate reduction rates on organic carbon consumption is demonstrated in Figure 7B which shows the total amount of organic carbon consumed as a percentage of the total available for each of the five simulations. Below a sulfate loading rate of 0.1 mol m^{-2} day^{-1} the slope of the curve is steep indicating that the amount of organic carbon consumed is highly dependent on the sulfate loading rate. This is due to the dependence of the sulfate reduction rate on sulfate concentrations at low sulfate loading rates (Figure 7A). At higher sulfate loading rates above 0.1 mol m^{-2} day^{-1} the total amount of organic carbon consumed approaches a maximum indicating that the consumption of organic carbon is insensitive to sulfate loading. This is because at high sulfate loading rates the sulfate concentrations remain high and the sulfate reduction rate remains near maximum throughout the column (Figure 7A). A similar trend is noted in the amount of sulfate reduced (Figure 7C) where the total number of moles of sulfate which are reduced through the duration of the simulations approaches a maximum as sulfate loading rates become greater than 0.1 mol m^{-2} day^{-1}. Although the maximum sulfate reduction rates are maintained with high rates of sulfate loading, the percentage of sulfate reduced, as a function of total sulfate loading (i.e. the total amount of sulfate entering the column through the duration of the simulations) is dramatically reduced (Figure 7C). This is because high sulfate concentrations are maintained throughout the column resulting in high levels of sulfate discharge.

Benner et al. (*12*) found that heterogeneity within the organic carbon reactive barrier produced zones with various rates of sulfate reduction. Along the fast flow paths sulfate concentrations remained high through the barrier thickness and sulfate reduction rates also remained near the maximum rate. Along the slow flow paths sulfate concentrations approached K_s and sulfate reduction rates declined through the barrier.

These results have important implications when assessing longevity and performance of the reactive material. For example, through the 14 month duration of the column experiments >27 pore volumes were pumped through the columns and the sulfate loading rates remained at or above ~0.1 mol m^{-2} day^{-1} indicating that the sulfate reduction rate would have remained near k_m. In this case therefore, the important parameter when determining the consumption of the organic matter is only the time over which the experiment was run, i.e. the organic carbon consumption could be expressed in units of moles per time. On the other hand, the number of pore volumes is somewhat arbitrary; an increase in the number of pore volumes pumped through the column would have resulted in no additional increase in organic carbon consumption.

The ability of the reactive mixture to remove ferrous iron is of primary importance to this remediation strategy. Furthermore, the form in which solid phase iron is stored may also have significant implications. The solubility of mackinawite is much lower than that of siderite. Therefore, mackinawite is the preferred iron sink in terms of providing a stable solid phase with minimal risk of dissolution at a later date. Data and simulations indicate that early in the experiments the predominant iron sink is siderite, which inhibits mackinawite precipitation. The precipitation of siderite does have the ability to remove larger amounts of iron, although this situation may be considered only temporary, as it will only continue as long as calcite dissolution occurs in the system. Later in the column life, once all the calcite had been exhausted, siderite no

longer precipitates to any significant extent and mackinawite becomes the predominant iron sink. At this point less iron is removed from solution. It is therefore apparent that Fe-removal at later times give a better indication of the long-term ability of the column to remediate acid mine drainage.

Acknowledgements

Funding for this research was provided by a Canadian Water Network grant awarded to David W. Blowes and Rejean Samson.

Literature Cited

(1) Dubrovsky, N.M., Morin, K.A., Cherry, J.A., and Smyth, D.J.A. *Water Pollut. Res. J. Can.* **1984**, 19, 55–89.

(2) Johnson, R.H., Blowes, D.W., Robertson, W.D., Jambor, J.L. *J. Contam. Hydrol.* **2000**, 41, 49-80.

(3) Benner, S.G., Blowes, D.W., and Ptacek, C.J. *Ground Water Monit. Remed.* **1997**, 17, 99 – 107.

(4) Ludwig, R.D., McGregor, R.G., Blowes, D.W., Benner, S.G., and Mountjoy, K. *Ground Water*, **2002**, 40, 59-66.

(5) Waybrant, K.R. *The prevention of acid mine drainage using in situ porous reactive walls: A laboratory study*. MSc. thesis, Dep. of Earth Sci., Univ. of Waterloo, Waterloo, Ont., Canada. **1995**.

(6) Waybrant, K.R., Ptacek, C.J., and Blowes, D.W. *Environ. Sci. Technol.* **2002**, 36, 1349-1356.

(7) Mayer, K. U., Frind, E. O., and Blowes, D. W. *Water Resour. Res.* **2002**, 38, 1174-1194.

(8) Benner, S. G., K. U. Mayer and D. W. Blowes, Abstract H22F-05, AGU Fall Meeting, San Francisco, California, December 13-17. **1999**.

(9) Mayer, K. U., Benner, S. G., Blowes, D. W., and Frind, E. O. In: *Sudbury '99, Conference on Mining and the Environment, Sudbury, Ontario* **1999**, Vol. 1, 145-154.

(10) Benner, S.G., Blowes, D.W., Gould, W.D., Herbert Jr, R.B., an Ptacek, C.J. *Environ. Sci. Technol.* **1999**, 33, 2793 –2799.

(11) Benner, S.G., Gould, W.D., and Blowes, D.W. *Chem.Geol.* **2000**, 169, 435 –448.

(12) Benner, S.G., Blowes, D.W., Ptacek, C.J., and Mayer, K.U. *Appl. Geochem.* **2002**, 17, 301-320.

(13) Herbert Jr, R.B., Benner, S.G., and Blowes, D.W. *Appl.Geochem.* **2000**, 15, 1331 –1343.

(14) Luther, G.W., and Church, T.M. In: *Sulfur cycling on the continents.* Eds. R.D. Howarth. J.W.B. Stewart and M.V. Ivanov. John Wiley & Sons Ltd. **1992**,

(15) Boudreau, B.P., and Westrich, J.T. *Geochim. Cosmochim. Acta* **1984**, 48, 2503-2516.

(16) Ball, J. W., and Nordstrom, D. K. *User's Manual for WATEQ4F, with revised thermodynamic database and test cases for calculating speciation of major, trace and redox elements in natural waters.* US Geological Survey, Open-File Report 91-183, 189 pp. plus diskette, **1991**.

(17) Allison, J.D., Brown, D.S., Novo-Gradac, K.J. *MINTEQA2/PRODEFA2, A geochemical assessment model for environmental systems: Version 3.0 Users's Manual.* U.S Environmental Protection Agency, EPA/600/3-91/021. **1991**.

(18) Westrich, J.T., and Berner, R.A. *Limnol. Oceanogr.* **1984**, 29, 236-249.

(19) Tarutis, W.J. Jr., and Unz, R.F. *Wat. Sci. Tech.* **1994**, 29, 219-226.

		Sulfate Reduction	Log k_{eff} (mol L^{-1} bulk s^{-1})	K_S mol L^{-1}
(1)	Reduction to sulfide	$CH_2O + 0.5SO_4^{2-} \rightarrow HCO_3^{2-} + 0.5H_2S + 1.5H^+$	6.5E-9	1.62E-3
		Mineral Precipitation/Dissolution Reactions		*Log K*
(2)	Mackinawite	$Fe^{2+} + HS^- \rightarrow FeS + H^+$	1.2E-11	4.6480
(3)	Siderite	$Fe^{2+} + CO_3^{2-} \rightarrow FeCO_3$	4.0E-8	10.4500
(4)	Calcite	$Ca^{2+} + CO_3^{2-} \rightarrow CaCO_3$	4.0E-8	8.4750
(5)	Gypsum	$Ca^{2+} + SO_4^{2-} \rightarrow CaSO_4$	4.0E-9	4.5800
(6)	Millerite	$Ni^{2+} + HS^- \rightarrow NiS + H^+$	1.2E-12	8.0420
(7)	Sphalerite	$Zn^{2+} + HS^- \rightarrow ZnS + H^+$	1.2E-12	11.6180

Table 1. Reaction Stoichiometries for sulfate reduction and mineral precipitation/dissolution reactions.

	Column 1	Column 2
Composted leaf mulch	19.5	23
Wood chips	8	0
Sawdust	10.5	22
Sewage sludge	10	0
Creek sediment	43	44
Agricultural limestone	2	3
Silica sand	7	8

Table 2. Composition of reactive mixtures used in column experiments expressed in wt. % (from Waybrant, 1995).

	Column 1	Column 2
Porosity	0.53	0.61
Hydraulic Conductivity	1.2E-5 ms^{-1}	1.2E-5 ms^{-1}
Diffusion Coefficient	1.0E-9 $m^2 s^{-1}$	1.0E-9 $m^2 s^{-1}$
Dispersivity	0.019 m	0.013 m
Flow Rate (0 – 65 days)	1.1E-7 m s^{-1}	1.1E-7 m s^{-1}
Flow Rate (> 65 days)	1.6E-7 m s^{-1}	1.88E-7 m s^{-1}

Table 3. Physical parameters used in the model. All parameters are values determined from column experiments (Waybrant, 1995).

Input Solution	Duration Column 1 (pore volume)	Duration Column 2 (pore volume)	pH	Alkalinity (mg/L $CaCO_3$)	SO_4 (mg/L)	Fe (mg/L)	Zn (mg/L)	Ni (mg/L)	Mn (mg/L)	Na (mg/L)	Ca (mg/L)	K (mg/L)	Mg (mg/L)	Br (mg/L)	Cl (mg/L)
Feed 0	0 - 4.7	0 – 5.9	N/A	N/A	1010	N/A	N/A	N/A	N/A	N/A	N/A	N/A	N/A	0	N/A
Feed 1	4.7 - 7.4	5.9 – 8.3	6.40	147.1	3210	694.4	0.72	0.94	9.75	46.8	506	27.4	242	26	14.19
Feed 2	7.4 - 9.2	8.3 – 10.1	5.85	54.8	3894	1181.0	0.95	1.40	12.87	50.0	99	31.7	320	0	482
Feed 3	9.2 – 12.0	10.1 – 12.9	6.41	45.0	3455	875.7	0.58	1.31	12.75	48.8	92	32.3	317	0	5.16
Feed 4	12.0 – 15.5	12.9 – 16.1	6.46	34.0	3660	956.3	0.97	12.28	19.80	48.8	83	29.2	288	N/A	7.71
Feed 5	15.5 – 18.4	16.1 – 18.7	6.60	25.9	2000	443.7	1.22	2.34	14.12	19.8	205	11.8	121	N/A	0.91
Feed 6	18.4 – 21.5	18.7 – 21.7	6.16	11.2	1623	379.4	0.85	1.60	8.96	14.1	214	7.9	83	N/A	15.43
Feed 7	21.5 – 24.9	21.7 – 24.8	6.61	27.8	1353	333.8	0.57	3.36	8.62	13.0	220	7.2	77	N/A	17.55
Feed 8	24.9 – 27.7	24.8 – 27.5	6.43	23.8	1400	316.3	N/A	N/A	N/A	N/A	N/A	N/A	N/A	N/A	14.43

Table 4. Input solution chemistry from column studies and used as boundary conditions for model (from Waybrant, 1995).

Figure Captions

Figure 1. Comparison of simulated (s) and observed effluent (eff) breakthrough for conservative Br tracer. Column data from Waybrant (1995).

Figure 2. Breakthrough curves of simulated (s) effluent aqueous component concentrations for SO_4, H_2S, and Fe(II) compared to observed influent (in) and effluent (eff) data for Column 1. The influent data has been shifted by one pore volume for comparison purposes. Column data from Waybrant (1995).

Figure 3. Simulated spatial profiles through Column 1 at; 150 days - A and B; 200 days – C and D; 300 days – E and F. A positive rate indicates precipitation while a negative rate indicates dissolution. The variable x is the distance along the column length. Dissolution/precipitation rates in mol L^{-1} bulk day^{-1}. SO_4 (in) is the corresponding column influent concentration assuming only advective flow.

Figure 4. Simulated (s) effluent aqueous component concentrations compared to influent (in) and effluent (eff) data for A) Ca and B) pH for Column 1. The influent data has been shifted by one pore volume for comparison purposes. Column data from Waybrant (1995).

Figure 5. Simulated spatial profiles through Column 1 at 200 days. A) Aqueous component concentrations of Ni and Zn. B) Dissolution/precipitation rates for millerite (NiS) and sphalerite (ZnS). The variable x is the distance along the column length.

Figure 6. Breakthrough curves of simulated (s) effluent aqueous component concentrations for SO_4, H_2S, and Fe(II) compared to observed influent (in) and effluent (eff) data for Column 2

with a sulfate reduction rate of A) 6.9 x 10^{-9} mol L^{-1} bulk day^{-1}; B) 1.5 x 10^{-8} mol L^{-1} bulk day^{-1}. The influent data has been shifted by one pore volume for comparison purposes. Column data from Waybrant (1995).

Figure 7. A) Simulated spatial profiles of sulfate reduction rates through Column 1 at 200 days for various water velocities. The variable x is the distance along the column length. B) Total organic carbon oxidized as a percentage as a percentage of the total available (in number of moles) for each of the five simulations shown in Figure 7A. C) Sulfate reduced and percent sulfate reduced vs. water velocity or sulfate loading rate. Percent sulfate reduces is calculated by ((total sulfate entering column+initial sulfate in column) – sulfate reduced) x100.

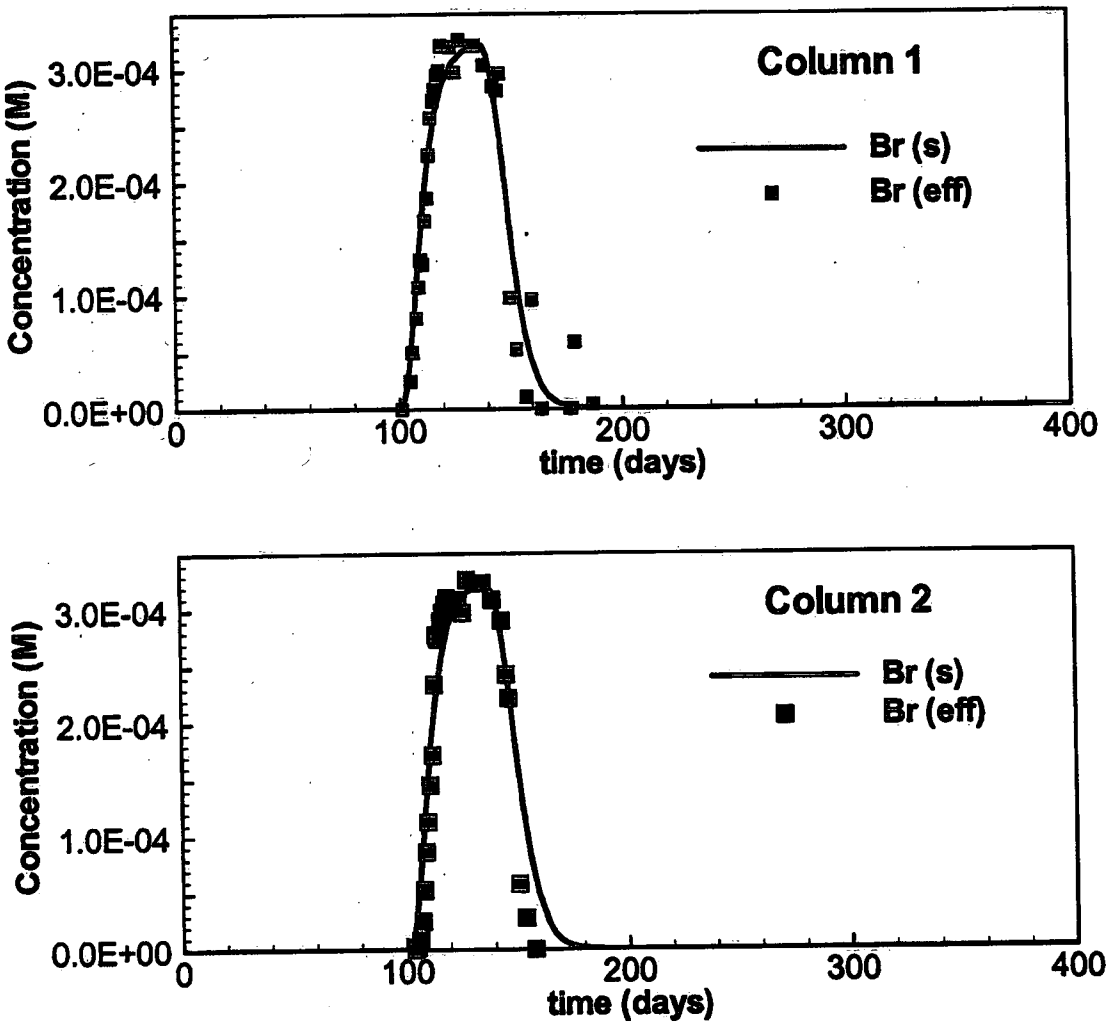
Column 1
Br (s)
Br (eff)
Concentration (M)
3.0E-04
2.0E-04
1.0E-04
0.0E+00
0
100
200
300
400
time (days)
Column 2
Br (s)
Br (eff)
Concentration (M)
3.0E-04
2.0E-04
1.0E-04
0.0E+00
0
100
200
300
400
time (days)

Figure 1.

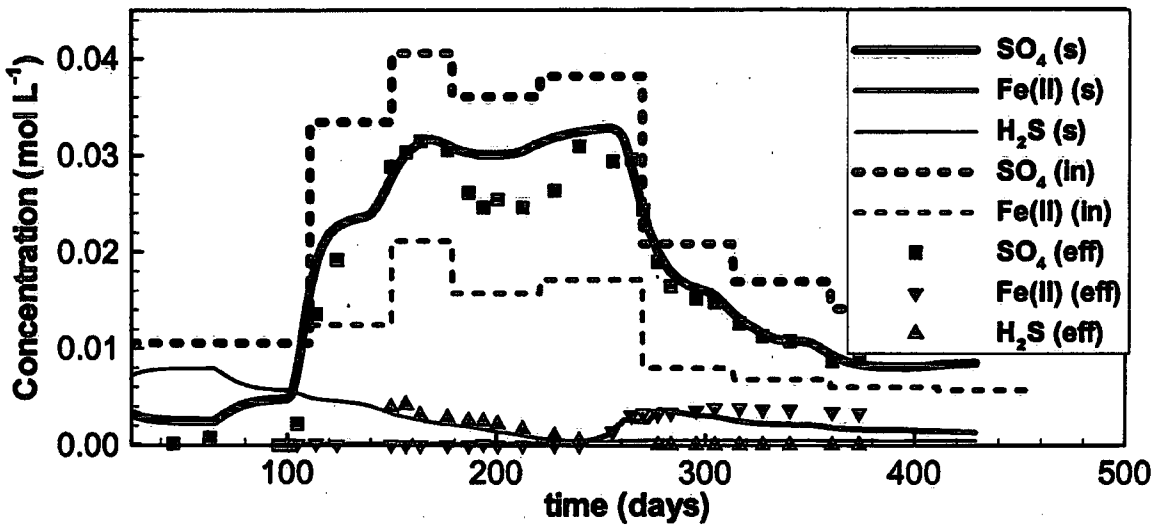
Concentration (mol L-1)
0.04
0.03
0.02
0.01
0.00
100
200
300
400
500
time (days)
SO4 (s)
Fe(II) (s)
H2S (s)
SO4 (in)
Fe(II) (in)
SO4 (eff)
Fe(II) (eff)
H2S (eff)

Figure 2.

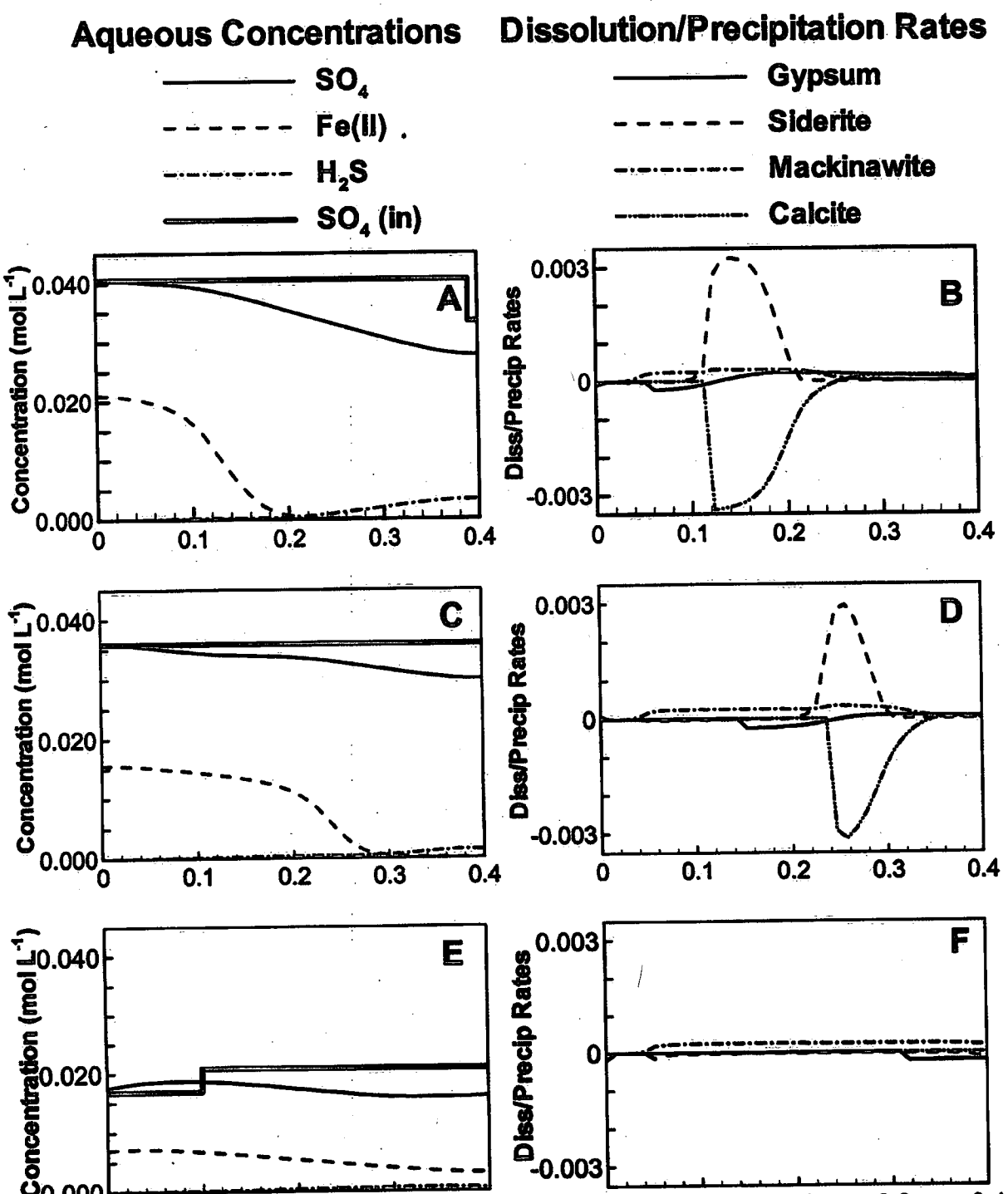
Aqueous Concentrations
Dissolution/Precipitation Rates
SO4
Fe(II)
H2S
SO4 (in)
Gypsum
Siderite
Mackinawite
Calcite
A
B
C
D
E
F
Concentration (mol L-1)
Diss/Precip Rates
0.040
0.020
0.000
0.003
0
-0.003
0
0.1
0.2
0.3
0.4
x (m)

Figure 3.

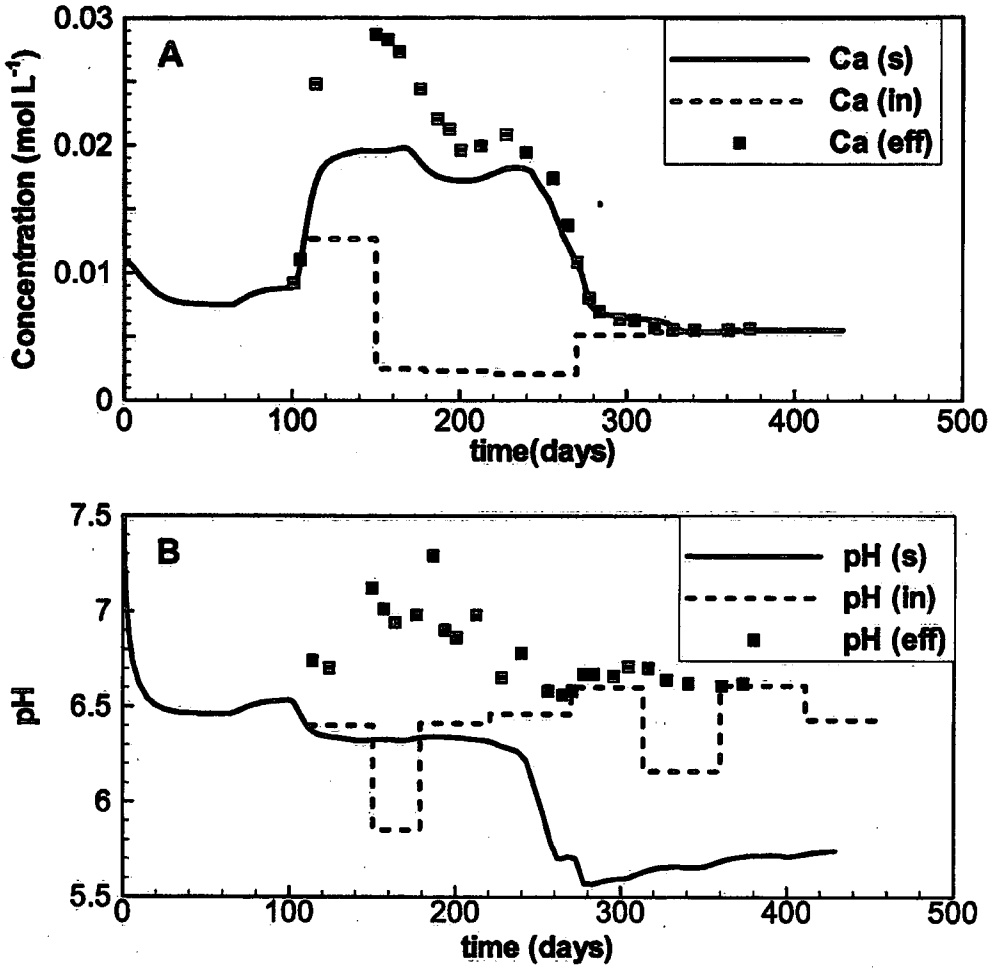
A
Ca (s)
Ca (in)
Ca (eff)
Concentration (mol L-1)
0.03
0.02
0.01
0
0
100
200
300
400
500
time(days)
B
pH (s)
pH (in)
pH (eff)
pH
7.5
7
6.5
6
5.5
0
100
200
300
400
500
time (days)

Figure 4.

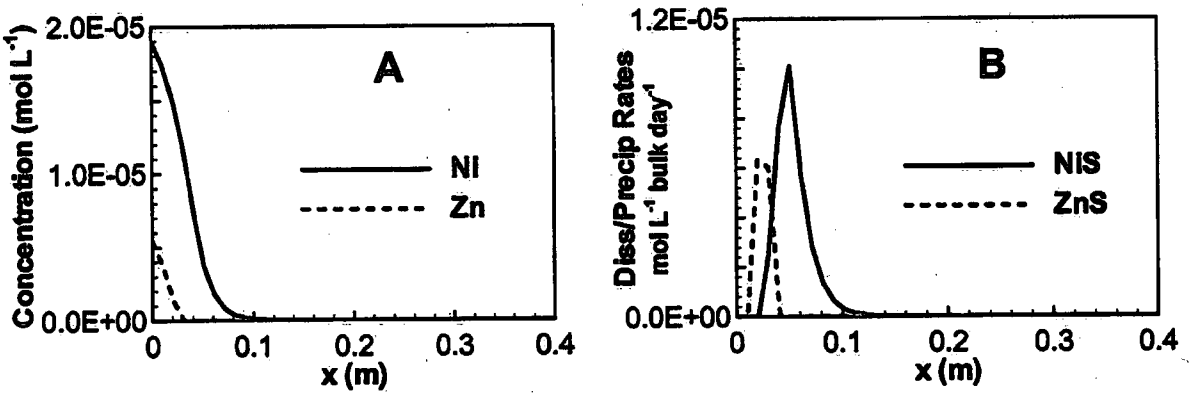
2.0E-05
1.0E-05
0.0E+00
Concentration (mol L-1)
A
Ni
Zn
0
0.1
0.2
0.3
0.4
x (m)
1.2E-05
0.0E+00
Diss/Precip Rates
mol L-1 bulk day-1
B
NiS
ZnS
0
0.1
0.2
0.3
0.4
x (m)

Figure 5.

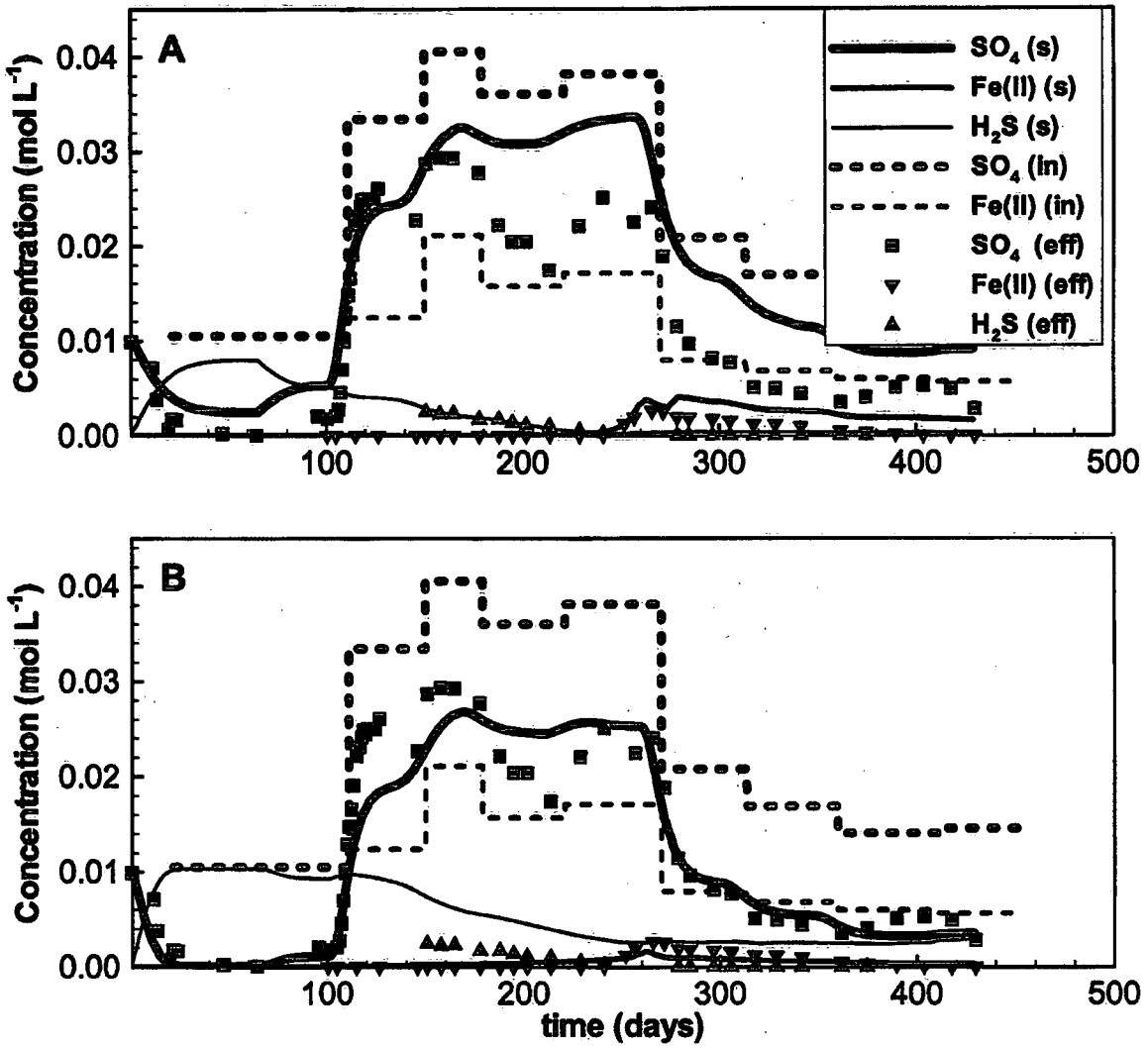
A
B
Concentration (mol L-1)
0.04
0.03
0.02
0.01
0.00
100
200
300
400
500
time (days)
SO4 (s)
Fe(II) (s)
H2S (s)
SO4 (in)
Fe(II) (in)
SO4 (eff)
Fe(II) (eff)
H2S (eff)

Figure 6.

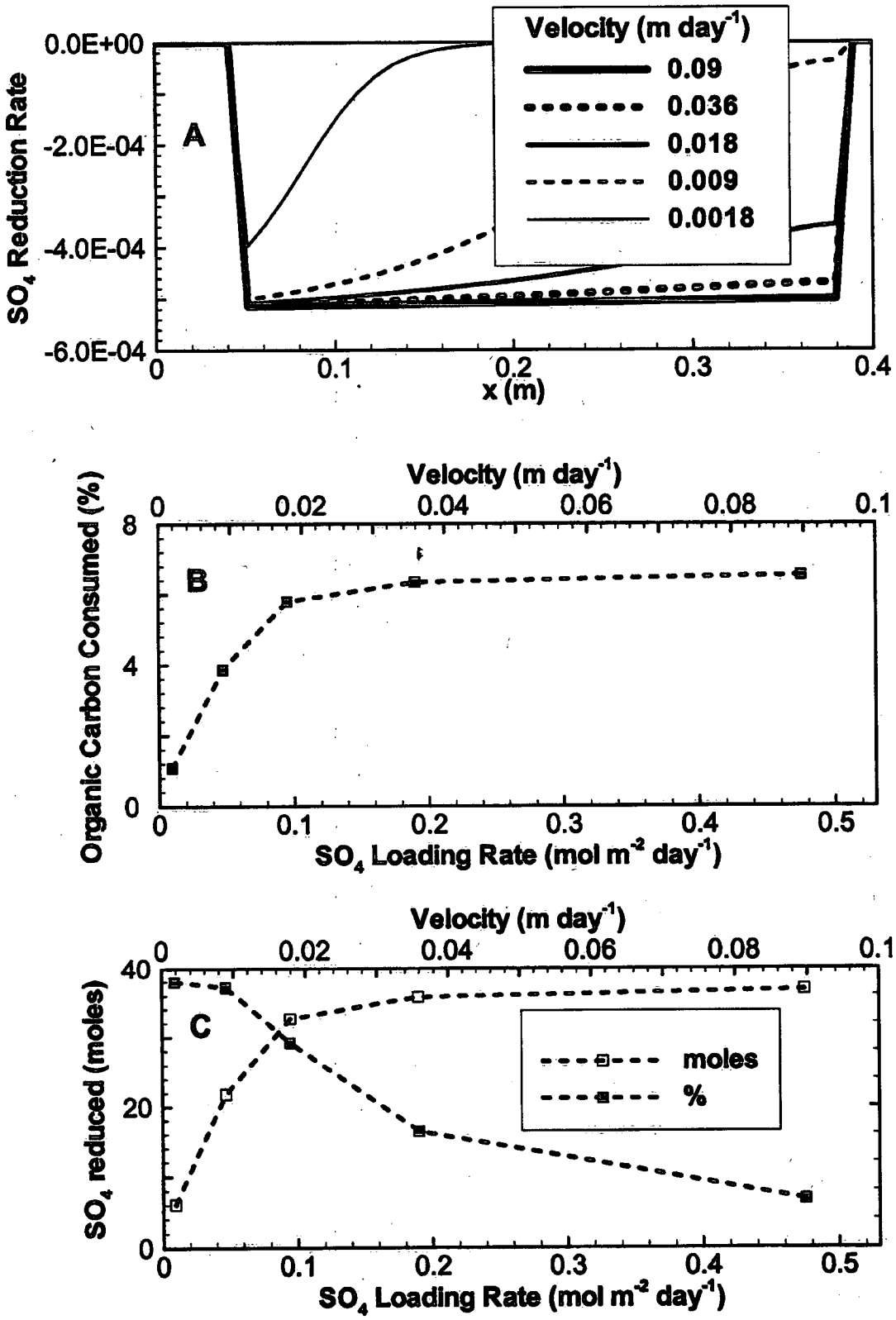
Velocity (m day-1)
0.09
0.036
0.018
0.009
0.0018
A
SO4 Reduction Rate
0.0E+00
-2.0E-04
-4.0E-04
-6.0E-04
0
0.1
0.2
0.3
0.4
x (m)
Velocity (m day-1)
0
0.02
0.04
0.06
0.08
0.1
B
Organic Carbon Consumed (%)
8
4
0
0.1
0.2
0.3
0.4
0.5
SO4 Loading Rate (mol m-2 day-1)
Velocity (m day-1)
C
SO4 reduced (moles)
40
20
0
moles
%
100
50
SO4 reduced (%)
SO4 Loading Rate (mol m-2 day-1)

Figure 7.

Environment Canada Environnement Canada

Canada

Canada Centre for Inland Waters
P.O. Box 5050
867 Lakeshore Road
Burlington, Ontario
L7R 4A6 Canada

National Hydrology Research Centre
11 Innovation Boulevard
Saskatoon, Saskatchewan
S7N 3H5 Canada

St. Lawrence Centre
105 McGill Street
Montreal, Quebec
H2Y 2E7 Canada

Place Vincent Massey
351 St. Joseph Boulevard
Gatineau, Quebec
K1A 0H3 Canada

Centre canadien des eaux intérieures
Case postale 5050
867, chemin Lakeshore
Burlington (Ontario)
L7R 4A6 Canada

Centre national de recherche en hydrologie
11, boul. Innovation
Saskatoon (Saskatchewan)
S7N 3H5 Canada

Centre Saint-Laurent
105, rue McGill
Montréal (Québec)
H2Y 2E7 Canada

Place Vincent-Massey
351 boul. St-Joseph
Gatineau (Québec)
K1A 0H3 Canada